TABLE I
PERCENT INHIBITION OF mRNA TRANSLATION BY 5'-TTGGGATAACACTTA-3'

15-mer	mRNA	
concentration, μM	VSV	BMV
5	23	ND (not done)
10	41	2
20	61	11
30	71	26
40	88	43
50	74	ND (not done)

300-500 ng aliquots of VSV mRNA on 1μg of BMV mRNA were translated in rabbit reticulocyte lysate; inhibition was calculated as a percentage of acid precipitable [^{35}S]Met cpm at 30 min. found in the absence of oligonucleotide, less blank without mRNA. Experiments were done at least twice, on different days.

greater than the predictions from the Fig. 2 structure. We presume that the oligonucleotide is competing with initiation factors and ribosomes for access to its target on the M mRNA. Further probing with an oligonucleotide complementary to the ribosome binding site, and with M gene antisense RNA of varying sizes may better identify susceptible and resistant portions of the M mRNA.

We thank Dr. John Patton for his help in isolating and translating VSV mRNA, Dr. Nick Muzyczka for synthesizing the oligonucleotide, and Dr. Michael Zuker for sending us a copy of RNAFLD.

This work was supported by an National Institutes of Health Biomedical Research Support grant, RR-07121, and an American Cancer Society Florida Division R. G. Thompson Summer Research Fellowship to I. Ruiz-Robles.

Received for publication 15 May 1985.

REFERENCES

1. Stephenson, M. L., and P. C. Zamecnik. 1978. Inhibition of Rous sarcoma viral RNA translation by a specific oligodeoxyribonucleotide. *Proc. Natl. Acad. Sci. USA.* 75:285–288.
2. Miller, P., C. Agris, L. Aurelian, K. Blake, T. Kelly, A. Murakami, M. P. Reddy, S. Spitz, P. Ts'o, and R. Wides. 1984. Inhibition of viral protein synthesis and infection by oligonucleoside methylphosphonates (ONMP). *Fed. Proc.* 43:1727.
3. Rose, J. K., and C. J. Gallione. 1981. Nucleotide sequences of the mRNA's encoding the vesicular stomatitis virus G and M proteins determined from cDNA clones containing the complete coding regions. *J. Virol.* 39:519–528.
4. Morrison, T. G., and H. F. Lodish. 1975. Site of synthesis of membrane and nonmembrane proteins of vesicular stomatitis virus. *J. Biol. Chem.* 250:6955–6969.
5. Patton, J. T., N. L. Davis, and G. W. Wertz. 1983. Cell-free synthesis and assembly of vesicular stomatitis virus nucleocapsids. *J. Virol.* 45:155–164.
6. Jacobson, A. B., L. Good, J. Simonetti, and M. Zuker. 1984. Some simple computational methods to improve the folding of large RNAs. *Nucl. Acids Res.* 12:45–52.
7. Borer, P. N., B. Dengler, and I. Tinoco, Jr. 1974. Stability of ribonucleic acid double-stranded helices. *J. Mol. Biol.* 86:843–853.
8. Beaucage, S. L., and M. H. Caruthers. 1981. Deoxynucleoside phosphoramidites. A new class of key intermediates for deoxypolynucleotide synthesis. *Tet. Lett.* 22:1859–1862.
9. Maxam, A. M., and W. Gilbert. 1980. Sequencing end-labeled DNA with base-specific chemical cleavages. *Methods Enzymol.* 65:499–561.
10. Laemmli, U. K. 1970. Clevage of structural proteins during the assembly of the head of bacteriophage T4. *Nature (Lond.).* 227:680–685.

ARCHITECTURE OF PRE-MESSENGER, NUCLEAR RIBONUCLEOPROTEIN MONOPARTICLES

J. WOOLEY,* S.-Y. CHUNG,‡ J. WALL,§ AND W. LESTOURGEON¶
**National Science Foundation, Washington, D.C. 20550; ‡National Institutes of Health, Bethesda, Maryland 20205; §Brookhaven National Laboratories, Upton, New York; and ¶Vanderbilt University, Nashville, Tennessee 37235*

Nascent pre-messenger RNA transcripts in eukaryotic nuclei are entirely associated with protein and organized into a series of globular particles spaced by thin ribonucleoprotein fibrils; the RNA is folded along these nuclear ribonucleoproteins, or nRNP, to achieve a packing ratio of at least 6:1–10:1 (1). Electron microscopic observations and biochemical studies on nRNP argue against a simple repeating structure similar to the chromatin fiber (1–3). Instead, electron micrographs of nascent transcripts suggest a gene-specific nRNP organization (1).

Brief ribonuclease digestion of purified mammalian nuclei releases individual RNP complexes or monoparticles, sedimenting broadly ~40S, that contain pre-messenger RNA (along with introns and other nRNA species) and a set of nucleus-restricted polypeptides. The six most abundant polypeptides species (constituting up to 90% of the total protein mass) have been termed A1 (molecular weight 32,000 d from SDS gels), A2 (34K), B1 (36K), B2 (37K), C1(42K), and C2 (44K), respectively (2). Our previous analyses suggest that A1, A2, and C1 are equimolar and are present at three times the abundance of B1, B2, and C2, which are also probably equimolar with each other (3).

We have used biochemical methods and the scanning transmission electron microscope (STEM) to begin a structural characterization of human (HeLa cell) monoparticles (isolated from purified nuclei following ribonuclease digestion: see references 2 and 3 for details of the

protocol). The monoparticles in our preparations contain RNA molecules 500–1,000 nucleotides in length and possess an 8:1 ratio of protein to RNA (3). Monoparticles appear in electron micrographs as globular, but somewhat irregular, complexes ~220 Å in diameter (Fig. 1). We have measured the mass of (unstained, freeze-dried, glutaraldehyde-fixed) monoparticles in the STEM (4). A very broad distribution, from ~0.7 million to over 2.5 million daltons, is observed; two classes of particles appear to be present, one with mass ~1.1 million and one ~1.8 million (after correction for glutaraldehyde contribution). If all particles maintain the same protein stoichiometry and protein/RNA ratio as observed for the total sample, this would correspond to one class of ~24 major polypeptides per monoparticle and one of ~36. Thus there must be a high copy number for the individual polypeptide species (up to 12 each of A1, A2, and C1 in the heaviest monoparticles routinely observed). The breadth and the specific range observed for the mass distribution is consistent with the sedimentation and chromatographic behavior of monoparticles (3) and may reflect the different types of particulate structures seen in nuclear spreads (1), although degredation during preparation may contribute. Nonetheless, the high copy number suggests the existence of polypeptide oligomers and a protein substructure.

Direct support of oligomeric interactions comes from experiments using reversible cross-linking reagents including dithiobisproprionimidate (DTBP), and the "zero-length" reagent (orthophenanthroline)$_2$Cu(II). Good yields of (A1)$_3$, (A2)$_3$, and (C1)$_3$ homotrimers are obtained, along with heterologous (A1-A2), (A1-A2)$_2$, (A2)$_n$(B1), where n = 1, 2, or 3, and (C1-C2) species. Table I presents an overview of our cross-linking results, indicating which specific polypeptides pairs are in close proximity in RNP. Presumably, those pairs joined by "zero-length" cross-linking reagents actually interact with each other. We have shown evidence elsewhere for the existence of stable (pure protein) (A2)$_3$(B1) tetramers free (in 0.6 M NaCl) solution (3).

TABLE I
SUMMARY OF CHEMICAL CROSSLINKING OF POLYPEPTIDES OBSERVED FOR ISOLATED RIBONUCLEOPROTEIN MONOPARTICLES

	A1	A2	B1	B2	C1	C2
A1	DC*	C				
A2	C	DC	DC			
B1		DC	D			
B2				D		
C1					DC	D
C2					D	D

*D indicates that the polypeptide pair can be crosslinked by 3,3'-dimethyl dithiobisproprionimidate; C indicated that the pair can be crosslinked by the complex (orthophenanthroline)$_2$Cu(II).

The relative distribution of mass thickness for a representative monoparticle is shown in Fig. 2. The mass distribution for nucleosomes is relatively flat, due to their disk-like structure and preferred orientation on carbon films (5, 6). However, nucleosomes exhibit more electron scattering from the outside of the particle since the DNA wraps around the histone core; similarly, cationic stains such as uranyl ions bind more extensively to the periphery (6). In contrast, RNP monoparticles are globular, roughly following a radial distribution expected for a ellipsoidal particle. Nor do they exhibit any obvious localization of the RNA even after staining with cations (data not shown). However, previous studies using nuclease and protease digestion suggest that the RNA lies on the outside of the particle, along with the C1 and A1 polypeptides (3).

The high polypeptide copy number, along with the existence of close contacts among the polypeptides and the existence of a protein tetramer free in solution, suggest that the monoparticle is built from a repeating oligomeric protein substructure. RNPs are quite different from ribosomes, and in a loose sense, are intermediate in organizational complexity between nucleosomes and small viruses. The electron micrographs suggesting a gene-specific architecture for nascent transcripts, and the qualitative and quantitative heterogeneity observed for monoparticles, suggest that there is more than one type of monoparticle. An elegant possibility is that unique transcripts arise by the

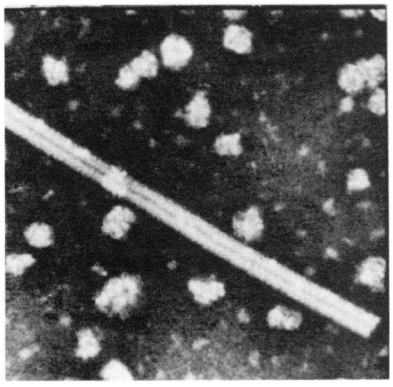

FIGURE 1 Isolated RNP monoparticles stained with Uranyl sulfate after fixation with 0.1% glutaraldehyde. TMV standard appears 180 Å wide as printed. Micrograph obtained with the Brookhaven STEM, which is supported by the National Institutes of Health Biotechnology Resources Program.

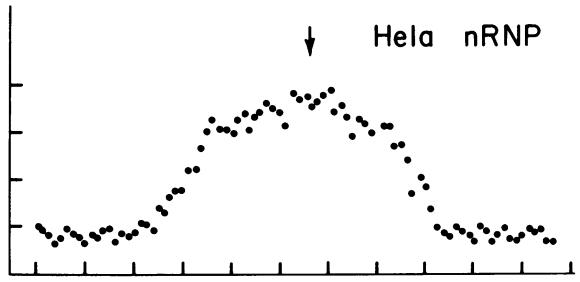

FIGURE 2 Line scan (normalized) across a representative RNP monoparticle. Horizontal bars are 20 Å apart.

gene-specific quantized or possibly combinatorial assembly of sets of discrete protein complexes. The unique distribution of sites of RNA secondary structure for each nuclear RNA molecule might underlie the organization, although other factors like pauses in transcription might also contribute. In sum, monoparticles appear to be built from complex oligomeric protein interactions that serve to fold the RNA and, given the dynamic role of nRNPs, may have important implications for RNA processing and transport.

Received for publication 30 May 1985.

REFERENCES

1. Beyer, A. L., O. L. Miller, and S. L. McKnight. 1980. Ribonucleoprotein structure in nascent hnRNA is on-random and sequence-dependent. *Cell.* 26:155–165.
2. Beyer, A. L., M. E. Christensen, B. W. Walker, and W. M. LeStourgeon. 1977. Identification and characterization of the packaging proteins of core 40S hnRNP particles. *Cell.* 11:127–138.
3. Lothstein, L., H. P. Arenstorf, S.-Y. Chung, B. W. Walker, J. C. Wooley, and W. M. LeStourgeon. 1985. General organization of protein in HeLa 40S nuclear ribonucleoprotein particles. *J. Cell Biol.* 100:1570d–1581.
4. Mossesson, M. W., J. Hainfeld, R. H. Haschemeyer, and J. Wall. 1981. Identification and mass analysis of human fibrinogen molecules and their domains by STEM. *J. Mol. Biol.* 153:691–718.
5. Langmore, J., and J. Wooley. 1975. Chromatin architecture: investigation of a subunit of chromatin by dark field electron microscopy. *Proc. Natl. Acad. Sci. USA.* 72:2691–2695.
6. Wooley, J., and J. Langmore. 1977. Electron microscopic studies on nucleosome structure. *In* Molecular Human Cytogenetics. R. S. Sparkes, D. Comings, and F. Fox, editors. Academic Press, New York. 41–55.

BINDING OF ETHIDIUM TO BACTERIOPHAGES T7 AND P22

G. A. GREISS, P. SERWER, AND P. M. HOROWITZ,
Department of Biochemistry, The University of Texas Health Science Center, San Antonio, Texas 78284

Bacteriophages P22 and T7 are genetically unrelated, but each contains a linear molecule of double-stranded DNA packaged within a capsid of protein. The capsid consists of an outer shell of icosahedrally arranged subunits, a projection (tail) from the exterior of the shell, and internal proteins (reviewed in reference 1). The outer radius of the capsid is 30.1 nm for T7 (2) and 31.4 nm for P22 (3). In the case of T7, the internal proteins form a cylinder coaxial with the tail (4). An internal cylinder has not been observed in P22. To detect changes in the conformation of DNA that occur as a consequence of packaging in T7's capsid, equilibrium binding of ethidium to packaged T7 DNA was compared to equilibrium binding of ethidium to DNA released from the T7 capsid (free DNA) (5). It was found that 1.2% of the packaged nucleotide pairs formed high affinity sites with an enthalpy of binding more negative than the enthalpy of binding to either the majority of packaged DNA nucleotide pairs or the nucleotide pairs of free DNA. The high affinity sites were revealed by curvature in Scatchard (6) plots of ethidium binding to packaged DNA. The role of T7's internal cylinder in producing the high affinity sites is not known. In addition, no study of the kinetics of ethidium's binding to packaged DNA has been made for either T7 or P22. Here we describe a study of the equilibrium binding of ethidium to P22, and the rates of ethidium's entry into T7 and P22.

RESULTS AND DISCUSSION

To determine whether or not the internal cylinder of T7 is required for the high-affinity binding sites, equilibrium binding of ethidium to P22 was quantitated using a Scatchard plot. It was found that the curvature produced by T7's high-affinity sites at a molar ratio of ethidium/nucleotide pairs (r) below 0.02 was also present for P22 (Fig. 1). Thus, the T7 component(s) required for the high affinity sites are apparently also present in P22. Therefore,

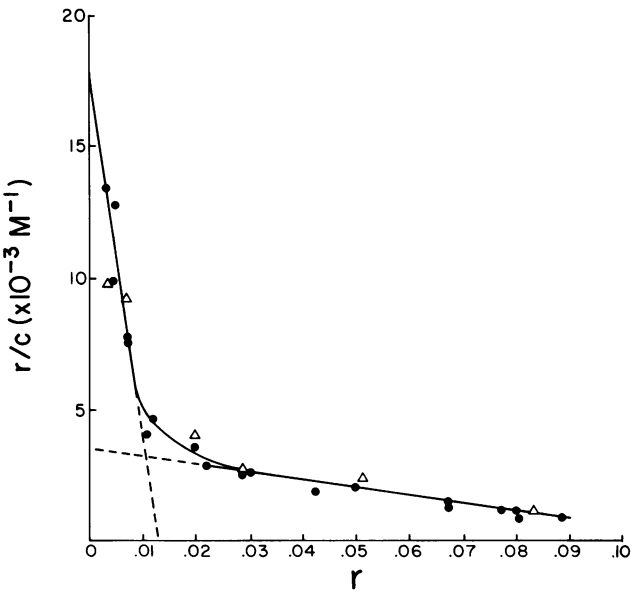

FIGURE 1 Binding isotherms for bacteriophages T7 and P22. Values of r/c at 25°C were plotted vs. r as previously described (6), where r is the molar ratio of bound ethidium to base pairs, and c is the concentration of unbound ethidium (●)-T7; (△)-P22.